Simulation of Stochastic Loads for Fatigue Experiments

by J.D. Sørensen and R. Brincker

ABSTRACT—A simple direct simulation method for stochastic fatigue-load generation is described in this paper. The simulation method is based on the assumption that only the peaks of the load process significantly affect the fatigue life. The method requires the conditional distribution functions of load ranges given the last peak values. Analytical estimates of these distribution functions are presented in the paper and compared with estimates based on a more accurate simulation method. In the more accurate simulation method samples at equidistant times are generated by approximating the stochastic load process by a Markov process. Two different spectra from two tubular joints in an offshore structure (one narrow banded and one wide banded) are considered in an example. The results show that the simple direct method is quite efficient and results in a simulation speed of about 3000 load cycles per second using a personal computer. Finally the proposed simulation method for fatigue-load generation is tested by comparing some fatigue damage measures obtained by the simulation methods.

Introduction

For structural systems where the fatigue failure mode is of importance, it is generally necessary to model the load on the structure as a stochastic process in order to give a realistic description of the load. For example, structures such as slender bridges, towers and offshore structures subjected to wind, sea waves or earthquakes are exposed to loads of distinctly stochastic nature. In this paper we assume the load to be modeled by stationary stochastic processes although one would quite seldom expect real loads to remain stationary during the whole lifetime of a structure. However, some quasi-stationary periods can usually be distinguished.

Besides the stochastic load, stochastic material properties also influence the lifetime of the so-called fatigue failure elements (potential fatigue failure areas). In the last decade there has been significant progress in the theoretical description of stochastic fatigue processes based on fracture mechanics, see, e.g., Madsen[1] and Sobczyk.[2] However, in order to use these models in practical problems it is necessary to perform experiments to get information about the material properties. Such experiments have to be performed with stochastic loads contrary to experiments up until now, which have almost all been performed with cyclic deterministic loads. Further, in order to study the fatigue processes under stochastic load in general, it is desirable to be able to perform experiments with stochastic loading.

J.D. Sørensen and R. Brincker are Assistant Professors, Institute of Building Technology and Structural Engineering, University of Aalborg, Sohngaardshomsvej 57, DK-9000 Aalborg, Denmark.

Original manuscript submitted: December 31, 1987. Final manuscript received: September 8, 1988.

In this paper the problem of simulating stochastic loads for experimental investigations is considered. In Brincker and Sørensen[3] another related problem is considered, namely the experimental problem of exposing a test specimen to the simulated load history. Assuming that we are not dealing with rate-sensitive problems (corrosion, creep, etc.) the problem is here to be able to apply the loads quickly enough to finish the test within a reasonable time (as fast as possible) being sure that the errors introduced by the load equipment do not significantly influence the test results. Results shown in Ref. 3 indicate that, using a simple computer-based control principle and the simple direct-simulation method described in this paper it is possible to perform fatigue experiments with simultaneous simulation at speeds up to about 150 load cycles per second without introducing any significant errors.

Two simulation methods are described in detail in this paper. The first and most accurate method is based on simulation of samples at equidistant times by approximating the stochastic load process by a Markov process. Simulation of a load realization by this method is relatively slow compared with the other simple direct method which is based on the assumption that only the peaks of the load process significantly affect the fatigue life. This simple direct method requires the conditional distribution functions of load ranges given the last peak values. Analytical approximations of these distribution functions are presented in the paper. The approximation introduced is that the first passage density function of the time between successive extremes of the load process is approximated by the density function of the time between zero crossings of the derivative process. The analytical estimates are compared with simulation results based on the more accurate simulation method for two different spectra from two tubular joints in an offshore structure (one narrow-banded spectrum and one wide-banded spectrum). Finally, the proposed simulation method for fatigue-load generation is tested by comparing some fatigue damage measures obtained by the two simulation methods.

Direct Simulation of Stochastic Loads for Fatigue Experiments

Realizations of stochastic processes (possible time histories corresponding to particular outcomes of the stochastic process) can be simulated in a number of different ways. In this paper we consider a stochastic process $\{Z(t)t \in T^*\}$, where T^* is the time index set. The process is assumed to be stationary and Gaussian with zero mean, unit standard deviation and a two-sided spectral density function $S_z(\omega)$, where ω is the cyclic frequency.

If the spectrum is approximated by a Fourier amplitude spectrum, realizations of the process can be generated by weighting a superposition of a large number of sinusoids at equispaced frequencies with randomly generated phase angles, Borgman[4] and Yang.[5] Another class of simulation methods which uses models formulated explicitly in discrete time is the autoregressive/moving average (ARMA) models. These models can be represented as stochastic linear-difference equations of finite order, Box and Jenkins,[6] Chang *et al.*[7] and Krenk and Clausen.[8] Closely related to ARMA models are methods formulated in continuous time, where realizations are generated at equidistant times, see, e.g., Franklin.[9,10] These methods generate outcomes of models which can be represented by stochastic differential equations of finite order, see the following section.

In order to reduce the total time for a fatigue experiment it is important to be able to simulate the stochastic load very quickly. If the spectrum has to be represented accurately the methods based on superposition of sinusoids generally require a large number of sinusoids. Therefore, it is not worthwhile generally to use these methods to generate stochastic fatigue loads when compared with the other methods mentioned above which are based on approximations of the load spectra by rational spectra of usually low order and only require relatively simple calculations to generate the realizations.

The above methods all generate realizations at equidistant times. However, most models of fatigue damage assume that the fatigue load can be represented by the ranges between successive extremes of the load process, see Fig. 1. This paper describes how fatigue loads can be generated by direct simulation of the extremes only. By this method a relatively coarse approximation $\{Y(t)\}$ to $\{Z(t)\}$ is generated, but examples indicate that the fatigue damage measures estimated from realizations by this method are only slightly different from measures obtained by using the more accurate simulation method based on solving linear-differential equations. As described in Ref. 3, a simulation method which only generates outcomes of the extremes of a stochastic process is easily incorporated in an adaptive control system for experimental tests.

Let v_i and p_i denote the values of the valley and the peak in the ith load cycle, see Fig. 2. v_i and p_i are generated from

$$v_i = p_i - e_i^p(p_i) \tag{1}$$

$$p_i = v_{i-1} + e_i^v(v_{i-1}) \tag{2}$$

where $e_i^p(p_i)$ and $e_i^v(v_{i-1})$ are realizations of conditional stochastic variables $E^p(p)$ and $E^v(v)$ modeling the range between successive extremes given the preceding peak or valley. By this approximation the influence of time is neglected. Simulation of $e_i^p(p_i)$ and $e_i^v(v_{i-1})$ requires information about the conditional distribution of ranges given the preceding extreme. This information can be obtained by analytical estimates of the conditional distribution functions or by simulation. In the following two sections it is shown how the simulation and the analytical estimates can be obtained.

Equations (1) and (2) can be considered as a Markov approximation of the stochastic process defined by the extremes of $\{Z(t)\}$. A further simplification is obtained if the dependence of the previous extreme is neglected in the model. In this case only the distribution of ranges is needed. On the other hand better approximations can be obtained if the ranges in eqs (1) and (2) are conditioned on more than just the previous extreme.

Due to symmetry of $\{Z(t)\}$ $E^p(p)$ and $E^v(v)$ can be modeled by a single stochastic variable $E(y)$. Realizations of $E(y)$ can be obtained using an inverse technique where realizations of independent stochastic variables uniformly distributed between 0 and 1 and the conditional distribution function of E given y are used. Realizations of independent and uniformly distributed variables can be generated by, e.g., the pseudorandom generators of the mixed-congruential type, see Hammersley.[11]

A practical implementation of the above method requires a discretization of the sample space of the stochastic process. Let $[-x_a, x_a]$ be the interval of interest. If this interval is divided into N subintervals simulation of realizations of the extremes by the above method requires estimation of a $N \times N$ matrix with elements specifying the conditional probability of a given range given an extreme. Based on this probability matrix a so-called jump matrix can be constructed. The ijth element in this matrix gives the jump e_{ij} to the next extreme given that the latest extreme was $x_a\left(j\frac{2}{N} - 1\right)$ (a valley) or $x_a\left(1 - j\frac{2}{N}\right)$ (a peak) and that the generated pseudorandom number is in the interval $\left[\frac{i-1}{N}, \frac{i}{N}\right]$. It is assumed that $e_{ij} \in \left\{k\frac{2x_a}{N}, k = 0,1,2,\ldots,N-1\right\}$.

Continuous Simulation by Markov Approximation Using Constant Time Step

In this section a simulation method is described which can be used to estimate the jump matrix used in the simple direct-simulation method and to evaluate the accuracy of the simple simulation method. The method, see Franklin[9,10] can be used to simulate realizations of a normal stationary stochastic process by approximating the stochastic process $\{Z(t)\}$ by a normal Markov process $\{X(t)\}$ which is characterized by the assumption that its spectral density can be written as

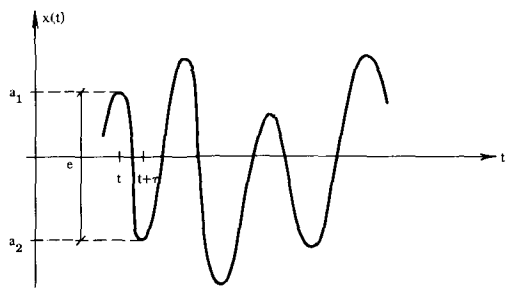

Fig. 1—Realization of $\{X(t)\}$

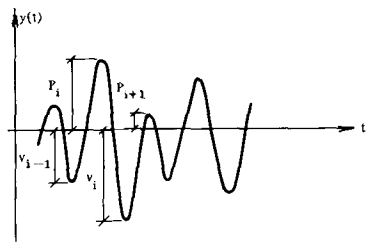

Fig. 2—Realization of load process

$$S_X(\omega) = \frac{1}{2\pi} \left| \frac{P(i\omega)}{Q(i\omega)} \right|^2 \tag{3}$$

where

$$P(i\omega) = p_0(i\omega)^m + p_1(i\omega)^{m-1} + \ldots + p_{m-1}(i\omega) + p_m \tag{4}$$

$$Q(i\omega) = (i\omega)^n + q_1(i\omega)^{n-1} + \ldots + q_{n-1}(i\omega) + q_n \tag{5}$$

S_X is assumed to be integrable which implies $n > m \geq 0$. Further the zeroes of Q have to fulfill $Re(i\omega) < 0$. From eq (3) it is seen that $\{X(t)\}$ can be obtained as the output from a linear system with frequency-response function $\frac{P(i\omega)}{Q(i\omega)}$ loaded by a white-noise process $\{F(t)\}$. The differential equations corresponding to this system can be written

$$X(t) = P\left(\frac{d}{dt}\right) \Gamma(t) \tag{6}$$

$$Q\left(\frac{d}{dt}\right) \Gamma(t) = F(t) \tag{7}$$

If realizations of $\Gamma(t)$, $\frac{d}{dt}\Gamma(t), \ldots, \frac{d^m}{dt^m}\Gamma(t)$ are known, realizations of $X(t)$ can be determined by eq (6). In Franklin[9,10] it is shown that realizations of the vector

$$\overline{\Gamma}(t) = \begin{pmatrix} \Gamma(t) \\ \Gamma^1(t) \\ . \\ . \\ . \\ \Gamma^{n-1}(t) \end{pmatrix} \tag{8}$$

can be obtained incrementally from

$$\overline{\Gamma}(t + \Delta t) = \overline{\overline{U}}(\Delta t)\overline{\Gamma}(t) + \overline{\overline{T}}\,\overline{W} \tag{9}$$

$\Gamma^j(t)$ denotes the jth derivative of $\Gamma(t)$. $\overline{\overline{U}}(\Delta t)$ and $\overline{\overline{T}}$ are matrices with elements depending on Δt and $q_1, q_2, \ldots, q_n$, see Franklin.[9,10] $\overline{W}$ is an n-dimensional vector of independent and normally distributed variables with mean zero and standard deviation one.

Given a spectrum $S_Z(\omega)$ an approximation $S_X(\omega)$ of the form eq (3) can be obtained by assuming n equal and solving a curve-fitting problem where the optimization variables $x_1, x_2, \ldots, x_{n+m+1}$ are connected to $\bar{p}$ and $\bar{q}$ as follows.

$$p_j = x_{n+1+j} \qquad j = 0,1,\ldots,m \tag{10}$$

$$q_j = (-1)^j \sum_{k_i < k_2 < \ldots < k_j} \prod_{l=1}^{j} (i\omega_{k_l}) \qquad j = 1,2,\ldots,n \tag{11}$$

$$\begin{aligned} \omega_1 &= x_1 + ix_2 \\ \omega_2 &= -x_1 + ix_2 \\ &\cdot \\ &\cdot \\ &\cdot \\ \omega_{n-1} &= x_{n-1} + ix_n \\ \omega_n &= -x_{n-1} + ix_n \\ \omega_{n+j} &= \omega_j^* \end{aligned} \tag{12}$$

where * denotes complex conjugate.

The curve-fitting problem is formulated as the optimization problem

$$\min_{\bar{x}} \int_0^\infty [S_Z(\omega) - S_X(\omega)]^2 \, d\omega \tag{13}$$

$$s.t.\ x_j > 0 \qquad j = 1,2,\ldots,n+m+1 \tag{14}$$

$$\varrho^0(0) = 1 \tag{15}$$

where

$$\varrho^m(\tau) = \int_{-\infty}^{\infty} (i\omega)^m S_X(\omega) e^{i\omega\tau} \, d\omega = 2\pi i \sum_{j=1}^{n} \cdot \frac{(i\omega_j)^m e^{i\omega_j\tau} \sum_{k=0}^{m} x_{n+m+1-k} (i\omega_j)^k \sum_{k=0}^{m} x_{n+m+1-k} (-i\omega_j)^k}{\prod_{\substack{k=1 \\ k\neq j}}^{2n} (\omega_j - \omega_k)} \tag{16}$$

is the mth derivative of the correlation coefficient function of $X(t)$. Equation (15) ensures that the standard deviation of $X(t)$ is 1. In the 'Example' section below, the optimization problem, eqs (13)–(15), is solved using the NLPQL algorithm developed by Schittkowski.[12]

In practice the procedure to generate a realization consists of the following steps. (a) Choose n and m. (b) Solve the optimization problem, eqs (13)–(15), to determine $\bar{p}$ and $\bar{q}$. (c) Compare $S_X(\omega)$ and $S_Z(\omega)$. If the approximation S_X is too good or too bad try new values of n and m and repeat step (b), or else go to step (d). (d) The matrices $\overline{\overline{U}}(\Delta t)$ and $\overline{\overline{T}}$ are determined, see Franklin.[9,10] (e) Initial values $\overline{\Gamma}(0)$ are determined, see Franklin.[9,10] (f) Given $\overline{\Gamma}(t)$ and a realization of $\overline{W}$ a new realization of $\overline{\Gamma}(t + \Delta t)$ is determined from eq (9). (g) A realization of $X(t + \Delta t)$ is determined using eqs (4) and (6):

$$X(t + \Delta t) = p_0\Gamma^m(t + \Delta t) + p_1\Gamma^{m-1}(t + \Delta t) \ \ldots + p_m$$

Steps (f) and (g) are repeated until the realization has the required length.

Distribution Functions of Ranges

This section describes how analytical estimates of the density function of ranges $f_E(e)$ and of the conditional distribution function of ranges given the previous extreme $F_E(e|q_1)$ can be obtained; see Fig. 1. The joint distribution function of a peak and a valley with time difference τ is defined by (see Madsen *et al.*[13])

$$f_{P,V}(a_1,a_2,\tau) = \frac{\int_{-\infty}^{0}\int_{0}^{\infty} -\ddot{x}_1\ddot{x}_2 f_{X_1X_2\dot{X}_1\dot{X}_2\ddot{X}_1\ddot{X}_2}(a_1,a_2,0,0,\ddot{x}_1,\ddot{x}_2)\,d\ddot{x}_1\,d\ddot{x}_2}{\int_{-\infty}^{0}\int_{0}^{\infty} -\ddot{x}_1\ddot{x}_2 f_{\dot{X}_1\dot{X}_2\ddot{X}_1\ddot{X}_2}(0,0,\ddot{x}_1,\ddot{x}_2)\,d\ddot{x}_1\,d\ddot{x}_2} \tag{17}$$

where $f_{X_1X_2\dot{X}_1\dot{X}_2\ddot{X}_1\ddot{X}_2}$ is the joint density function of X_1, X_2, $\dot{X}_1$, $\dot{X}_2$, $\ddot{X}_1$ and $\ddot{X}_2$. Further $X_1 = X(t)$ and $X_2 = X(t + \tau)$. The derivatives $\dot{X}$ and $\ddot{X}$ are assumed to exist. In the appendix it is shown how eq (17) can be calculated.

In order to estimate the density function of the range between two successive extremes it is also necessary to estimate the density function of times T between successive extremes, $f_T(\tau)$. This is a first passage problem which cannot generally be solved analytically. A simple estimate

of $f_T(\tau)$ can be obtained by using the upper bound,

$$f_T(\tau) \leq \int_{-\infty}^{0} \int_{0}^{\infty} -\ddot{x}_1 \ddot{x}_2 f_{\dot{x}_1 \dot{x}_2 \ddot{x}_1 \ddot{x}_2}(0,0,\ddot{x}_1,\ddot{x}_2) d\ddot{x}_1 \, d\ddot{x}_2 \tag{18}$$

Equation (18) is used in the interval $0 \leq \tau \leq T_0$ where T_0 is determined from the normalization condition

$$\int_0^{T_0} f_T(\tau) d\tau = 1 \tag{19}$$

When $\tau > T_0$ we use $f_T(\tau) = 0$.

From eqs (17) and (18) the density function f_E of the range between two successive extremes can be estimated by

$$f_E(e) = \int_0^{\infty} f_T(\tau) \int_{-\infty}^{\infty} f_{P,V}(a, a-e, \tau) da \, d\tau \tag{20}$$

Equation (20) can be calculated by numerical integration. The distribution function $F_E(e|a_1)$ of the range E given the peak a_1 is estimated from

$$F_E(e|a_1) = \frac{\int_{-\infty}^{e} \int_{0}^{\infty} f_{P,V}(a_1, a_1 - x, \tau) f_T(\tau) d\tau dx}{f_P(a_1)} \tag{21}$$

In eq (21) the density function $f_P(a)$ of a single peak is given by

$$f_P(a) = \frac{\int_{-\infty}^{0} -\ddot{x} f_{X\dot{X}\ddot{X}}(a, o, \ddot{x}) d\ddot{x}}{\int_{-\infty}^{0} -x f_{\dot{X}\ddot{X}}(o, \ddot{x}) d\ddot{x}} = -\frac{\sqrt{R}}{\sqrt{\varrho^4(0)}} \exp\left(-\frac{1}{2}a^2\right) \int_{-\infty}^{-\frac{a\varrho^2(0)}{\sqrt{R}}} \cdot \left(y + \frac{a\varrho^2(0)}{\sqrt{R}}\right) \varphi(y) dy \tag{22}$$

where

$$R = \varrho^4(0) - [\varrho^2(0)]^2 \tag{23}$$

and $\varphi(\cdot)$ is the normalized normal density function.

As described in 'Direct Simulation of Stochastic Loads for Fatigue Experiments' above, eq (21) can be used as the basis of simulation of successive extremes of a fatigue load in process. If the influence of the latest extreme on the range is neglected, eq (20) can be used as the basis of the simulation.

Example

In this example we consider two tubular joints in a three-dimensional model of an offshore steel-jacket platform analyzed in Sigurdsson.[14] The structure is loaded mainly by waves with frequencies about $\omega = 0.6$ [rad/s] and has the lowest eigenfrequency $\omega_1 = 3.0$ [rad/s]. In Figs. 3 and 4, the stress spectra are shown for the two joints for two different load cases. The spectra are normalized to unit standard deviation. Estimates of the spectra are calculated in Sigurdsson[14] at a number of discrete frequencies and are shown in the figures as vertical lines. Also shown are approximations of the spectra by rational spectra, see eq (3). The rational spectra are shown by continuous lines. In both spectra $n = 8$ and $m = 3$ are used. The spectra are characterized by the parameter ϵ defined by

$$\epsilon = \sqrt{1 - \frac{m_2^2}{m_0 m_4}} \tag{24}$$

where m_j is the jth spectral moment

$$m_j = 2 \int_0^{\infty} \omega^j S(\omega) d\omega \tag{25}$$

ϵ close to 0 and 1 indicate a narrow-banded and a wide-banded spectrum, respectively. The spectra in Figs. 3 and 4 have $\epsilon = 0.2$ and $\epsilon = 0.8$. Therefore, they can be characterized as 'narrow' and 'wide', respectively.

In Figs. 5 and 6, estimates of the density function f_T of times between successive extremes are shown by continuous lines. The estimates are calculated using the approximation eq (18) and the approximate rational spectra. Also shown in Figs. 5 and 6 are simulation estimates. The simulations are performed using the method described in 'Constant

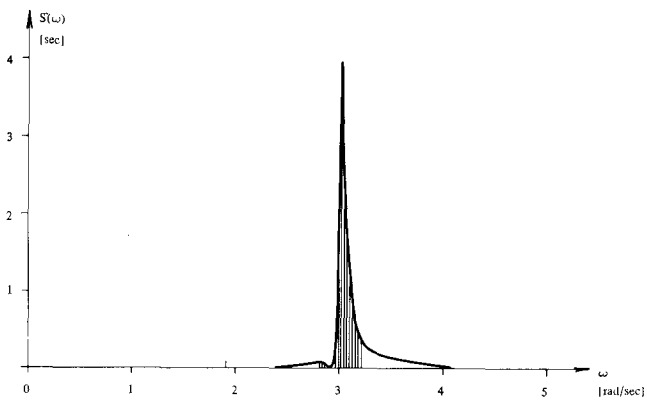

Fig. 3—Spectral density function for a stochastic process with a 'narrow' spectrum. The vertical lines show estimates from Sigurdsson[14] and the continuous line shows the approximation by a rational spectrum with $n = 8$ and $m = 3$ ($\epsilon = 0.2$)

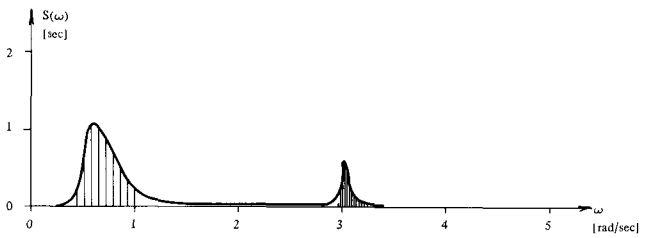

Fig. 4—Spectral density function for a stochastic process with a 'wide' spectrum. The vertical lines show estimates from Sigurdsson[14] and the continuous line shows the approximation by a rational spectrum with $n = 8$ and $m = 3$ ($\epsilon = 0.8$)

Simulation by Markov Approximation Using Constant Time Step' above with $\Delta t = 0.1$ s and a total simulated time length of 60000 s. It is seen that in both figures the deviations are small between the upper bound eq (18) with cut-off at T_0 and the simulation results.

In Figs. 7 and 8, analytical estimates of the conditional distribution function $F_E(e|a^l \le a_1 \le a^u)$ calculated using eq (21) are compared with simulation results. Four different intervals of the previous extreme are considered. Figure 7 shows that in the case of a narrow-banded spectrum the analytical estimates correspond very well to the simulation results. For the wide-banded spectrum Fig. 8 shows that some deviation occurs for distributions conditioned on high previous extremes.

In Figs. 9 and 10, estimates of the density function $f_E(e)$ of ranges between successive extremes calculated using eq (20) are compared with simulation results. • indicates simulation estimates of the density function of ranges between successive extremes. Also shown in the figures are simulation results indicated by ×. These estimates are based on ranges obtained by performing Rainflow counting, see Madsen *et al.*[13] Rainflow counting is generally accepted to give good estimates of the density functions of ranges and expected number of ranges to be used in practical fatigue analyses. For a narrow-band

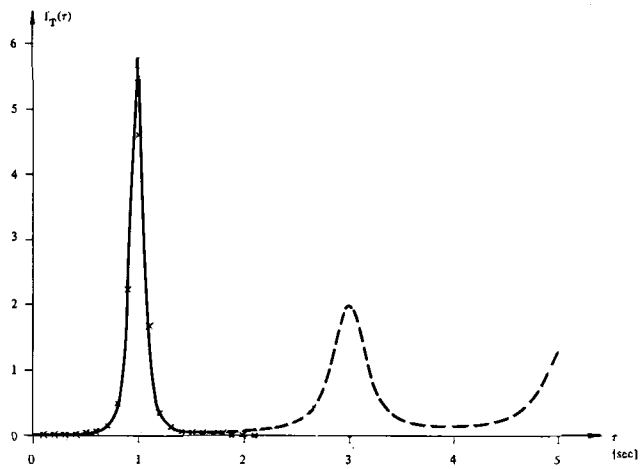

Fig. 5—Density function $f_T(\tau)$ of times between extremes estimated by eq (18) for a stochastic process with a 'narrow' spectrum. The start of the broken line indicates the time, T_0, see eq (19). Simulation results are indicated by x

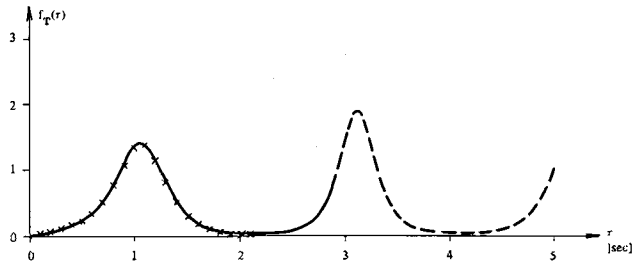

Fig. 6—Density function $f_T(\tau)$ of times between extremes estimated by eq (18) for a stochastic process with a 'wide' spectrum. The start of the broken line indicates the time, T_0, see eq (19). Simulation results are indicated by x

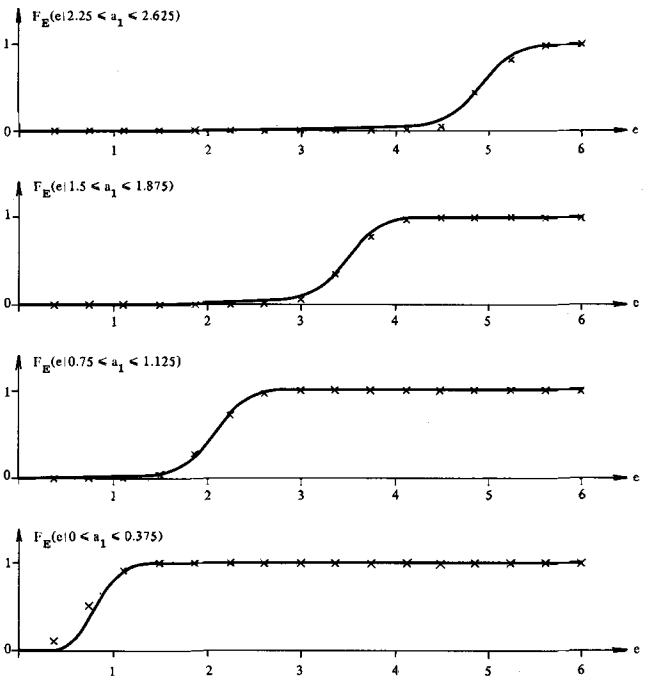

Fig. 7—Conditional distribution functions $F_E(e|a^l \le a_1 \le a^u)$ of range E given an extreme a_1 estimated by eq (21) for a stochastic process with a 'narrow' spectrum. Simulation results are indicated by x

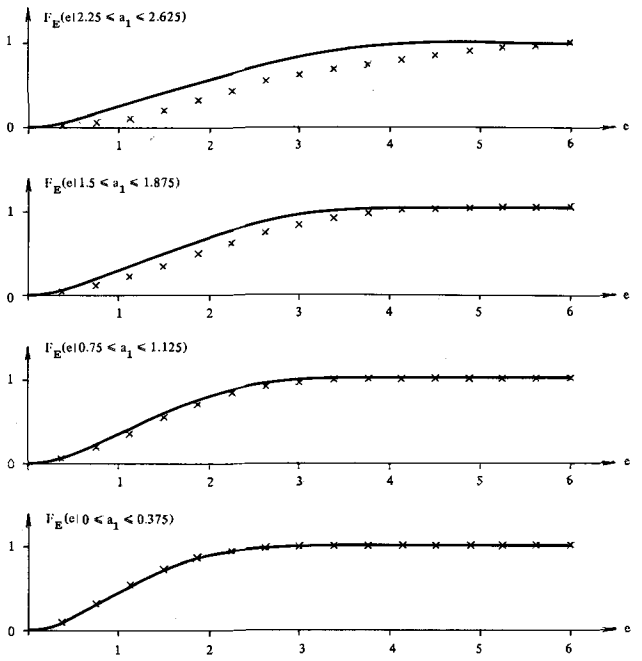

Fig. 8—Conditional distribution functions $F_E(e|a^l \le a_1 \le a^u)$ of range E given an extreme a_1 estimated by eq (21) for a stochastic process with a 'wide' spectrum. Simulation results are indicated by x

process the range counting and the rainflow counting methods become equivalent. Therefore the density functions f_E should give the same results. This is also seen from Fig. 9. Furthermore it is seen that there is very close agreement between analytical estimates and simulation results. For the wide-banded spectrum the estimates based on rainflow counting are significantly different from the analytical estimates and the simulation estimates based on range counting.

In order to investigate the simple direct-simulation method for fatigue tests proposed in 'Direct Simulation of Stochastic Loads for Fatigue Experiments' above some simulations have been performed using this method. Only extremes within the interval $[-3,3]$ have been considered. The interval has been discretized into 16 uniformly distributed points. It is then possible to estimate a jump matrix (see 'Direct Simulation . . .' above) with 16×16 elements. Each of the elements gives the range to the next extreme given an extreme (peak or valley). Each of the elements are estimated by simulation.

In Figs. 11 and 12, simulation results obtained by the simple direct-simulation method are shown. o and + indicate estimates of the density of ranges between successive extremes and estimates based on rainflow counting. For the narrow-band spectrum there are only small differences between the estimates obtained by the two methods. The results for the wide-banded spectrum show greater differences between the estimates of the two simulation methods. But still the differences are not significant (see also Figs. 13-20). The differences are most obvious for the rainflow counting estimates and are most probably due to the fact that the simple simulation method is not able to reproduce realizations where the next extreme is dependent on more than the last extreme.

Finally the simple direct-simulation method to be used to generate load realizations in fatigue experiments is tested by comparing the fatigue lives of a simple model. Let a and N model the crack length and the number of stress ranges. Then in linear-elastic fracture mechanics the increase in crack length Δa for each load cycle can in

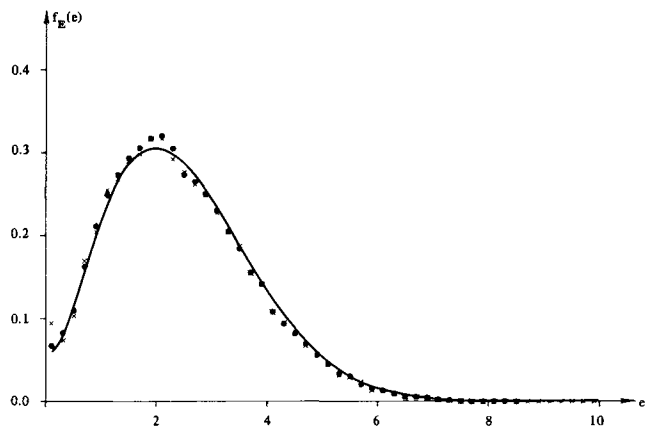

Fig. 9—Density function $f_E(e)$ of range between extremes estimated by eq (20) for a stochastic process with a 'narrow' spectrum. Simulation results are indicated by • and x

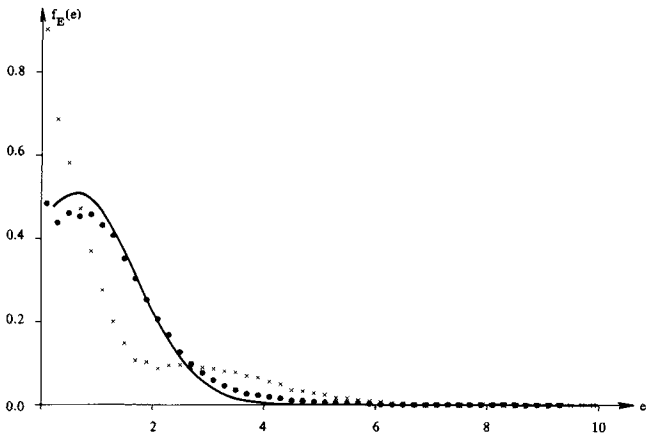

Fig. 10—Density function $f_E(e)$ of range between extremes estimated by eq (20) for a stochastic process with a 'wide' spectrum. Simulation results are indicated by • and x

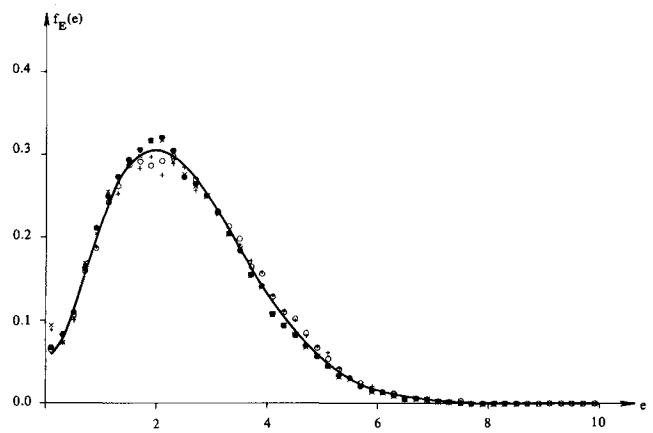

Fig. 11—Density function $f_E(e)$ of range between extremes estimated by eq (20) for a stochastic process with a 'narrow' spectrum. Simulation results are indicated by •, x, o and +

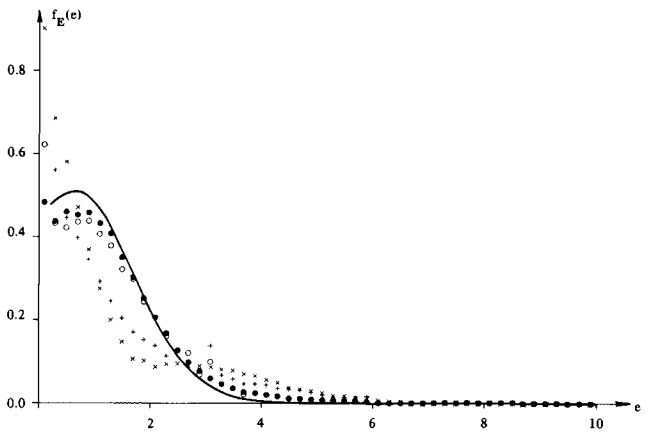

Fig. 12—Density function $f_E(e)$ of range between extremes estimated by eq (20) for a stochastic process with a 'wide' spectrum. Simulation results are indicated by •, x, o and +

some simple cases be determined by (see Madsen *et al.*[13])

$$\Delta a = c(b\Delta\sigma\sqrt{\pi a})^{m_1} \tag{26}$$

where c and m_1 are material parameters. b is a constant and $\Delta\sigma$ is the range between successive extremes of the load process. c, m_1 and b are assumed to be deterministic. The initial length and the critical crack length are modeled by a_0 and a_{cr}. In the following example we use $c = 1.93\ 10^{-13}$, $m_1 = 3$, $b = 100$, $a_0 = 2$ and $a_{cr} = 50$ (dimensions omitted).

In Figs. 13-20 simulation results show the crack length as a function of the number of load cycles. Both the range and the rainflow counting methods are used to determine the load cycles to be used in eq (26). However, it should be noted that using the rainflow counting method does not have a direct physical meaning when the load cycles are used in the crack-growth model, eq (26). For the narrow-banded spectrum it is seen that the same critical number of load cycles N_{cr} is obtained for the 'exact' simulation method described above and the simple-direct simulation method proposed both for range and rainflow counting based methods. Each figure is based on 25 simulations. Figures 17-20 show the results for the wide-banded spectrum based on ten simulations. The results show that significant differences for N_{cr} are obtained for the range and rainflow counting method, but the two simulation methods give nearly the same estimates. From these crack-length simulations it can be concluded that the simple direct fatigue load simulation method is able to produce realizations which result in nearly the same fatigue life as realizations simulated using the much more advanced simulation method described in 'Continuous Simulation by Markov Approximation Using Constant Time Step'. If the single crack-length realizations are compared the same conclusion can be drawn. In addition it appears from the realizations that the narrow-banded spectrum results in much more fluctuating realizations than the wide-banded spectrum.

In Table 1 the critical numbers of load cycles N_{cr} are shown for 'exact' simulation and 'simple' simulation for different discretizations $N = 8, 16$ and 32. All estimates are based on 25 realizations. From the table it appears that increasing the discretization degree in the simple

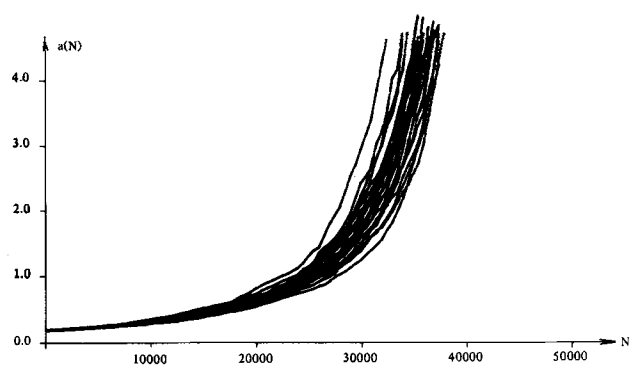

Fig. 13—Crack length a as a function of the number of load cycles N for a stochastic process with a 'narrow' spectrum. 'Exact simulation' and range counting are used ($E[N_{cr}] = 36300$ and $\sigma[N_{cr}] = 1300$)

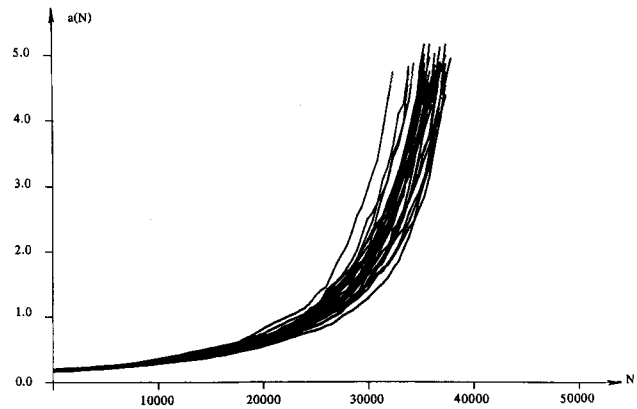

Fig. 14—Crack length a as a function of the number of load cycles N for a stochastic process with a 'narrow' spectrum. 'Exact simulation' and rainflow counting are used ($E[N_{cr}] = 36200$ and $\sigma[N_{cr}] = 1300$)

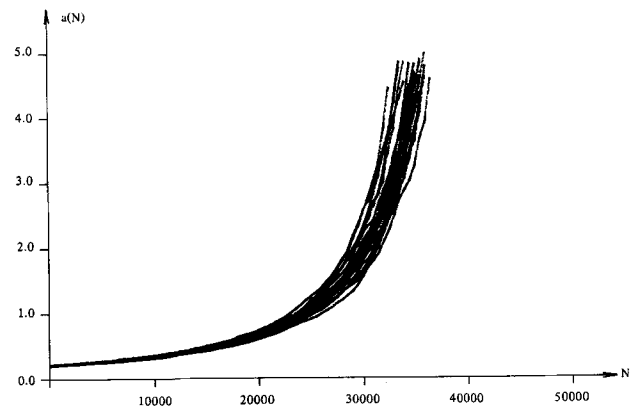

Fig. 15—Crack length a as a function of the number of load cycles N for a stochastic process with a 'narrow' spectrum. 'Simple simulation' and range counting are used ($E[N_{cr}] = 35200$ and $\sigma[N_{cr}] = 900$)

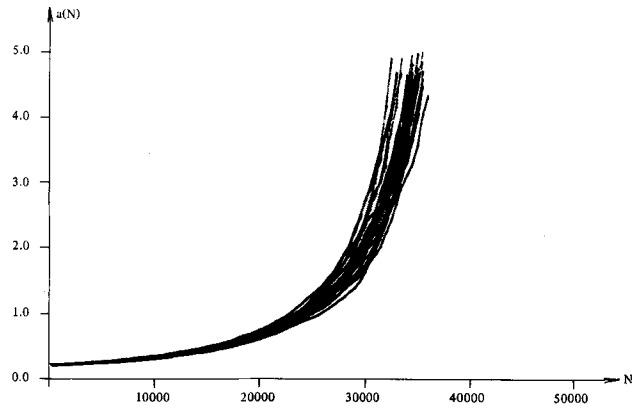

Fig. 16—Crack length a as a function of the number of load cycles N for a stochastic process with a 'narrow' spectrum. 'Simple simulation' and rainflow counting are used ($E[N_{cr}] = 34800$ and $\sigma[N_{cr}] = 900$)

TABLE 1—NUMBER OF LOAD CYCLES N_{cr} CORRESPONDING TO FAILURE

	Rainflow Counting		Range Counting	
	μ	σ	μ	σ
'Narrow' spectrum				
'Exact' simulation	36200	1300	36300	1300
'Simple' simulation, N = 8	40000	600	41300	650
'Simple' simulation, N = 16	34800	900	35200	900
'Simple simulation, N = 32	36000	570	37100	600
'Wide' spectrum				
'Exact' simulation	83100	1250	152000	1830
'Simple' simulation, N = 8	124200	770	194600	1130
'Simple' simulation, N = 16	100300	680	161000	830
'Simple' simulation, N = 32	94700	600	152700	750

μ = *expected value*, σ = *standard deviation.*

direct-simulation method generally implies that the estimates of N_{cr} approach the estimates obtained by 'exact' simulation. A discretization with N = 32 is seen to give satisfactory results in most cases.

Conclusion

In this paper an efficient and simple method to simulate realizations of stochastic loads for fatigue experiments is presented. The method is based on the assumption that for most fatigue experiments it is sufficient to describe the realizations by the extreme values of the load. A simple method is proposed where the range between two successive extremes is assumed only to depend on the value of the latest extreme. Realizations can thus be generated if the conditional distribution function of the range given the latest extreme is known.

Two methods to estimate the conditional distribution function are described. The first method is based on an analytical approximation to the first-passage problem which it is necessary to solve to estimate the conditional distribution function. Numerical examples indicate that

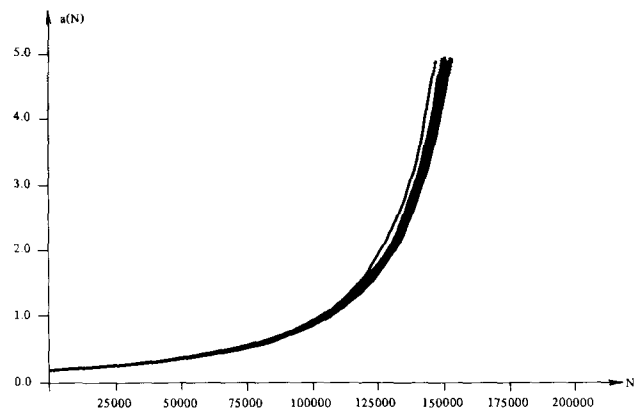

Fig. 17—Crack length a as a function of the number of load cycles N for a stochastic process with a 'wide' spectrum. 'Exact simulation' and range counting are used ($E[N_{cr}]$ = 152000 and $\sigma[N_{cr}]$ = 1830)

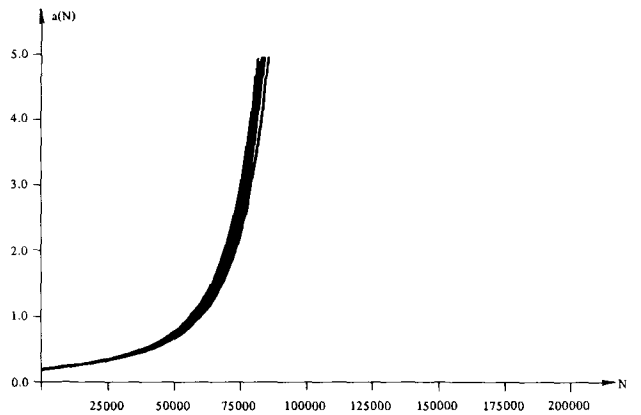

Fig. 18—Crack length a as a function of the number of load cycles N for a stochastic process with a 'wide' spectrum. 'Exact simulation' and rainflow counting are used ($E[N_{cr}]$ = 83100 and $\sigma[N_{cr}]$ = 1250)

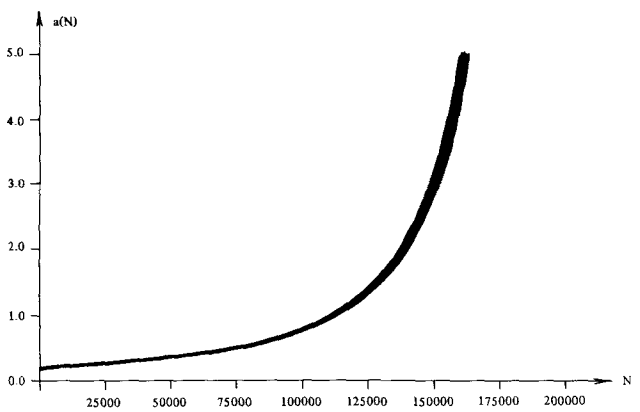

Fig. 19—Crack length a as a function of the number of load cycles N for a stochastic process with a 'wide' spectrum. 'Simple simulation' and range counting are used ($E[N_{cr}]$ = 161000 and $\sigma[N_{cr}]$ = 830)

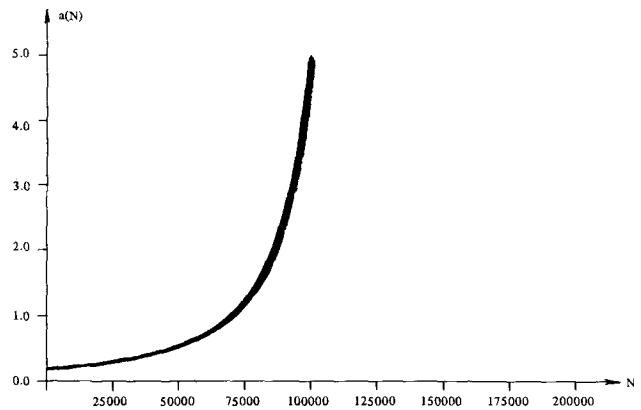

Fig. 20—Crack length a as a function of the number of load cycles N for a stochastic process with a 'wide' spectrum. 'Simple simulation' and rainflow counting are used ($E[N_{cr}]$ = 100300 and $\sigma[N_{cr}]$ = 680)

for two stochatic processes described by quite different spectra the approximation gives results which agree well with simulation results. The second method is based on estimates determined from a more accurate simulation method which is based on a Markov approximation of the spectrum of the stochastic process describing the fatigue load.

The simple fatigue load simulation method is compared with the more accurate simulation method in an example where the fatigue-crack-length growth is described by a simple model. The example shows that the simple simulation method for the two spectra considered is able to describe the fatigue crack growth with sufficient accuracy.

Acknowledgments

Financial support from the Danish council for Scientific and Industrial Research is gratefully acknowledged.

References

1. Madsen, H.O., "Deterministic and Probabilistic Models for Damage Accumulation Due to Time Varying Loading," DIALOG 5-82, Danish Eng. Academy, Lyngby, Denmark (1982).
2. Sobczyk, K., "Modelling of Random Fatigue Crack Growth," Eng. Fract. Mech., **24** (4), 609-623 (1986).
3. Brincker, R. and Sorensen, J.D., "High Speed Fatigue Stochastic Testing," submitted to EXPERIMENTAL MECHANICS.
4. Borgman, L.E., "Ocean Wave Simulation for Engineering Design," J. Waterways and Harbours Division, ASCE, **95** (WW4), 557-583 (1969).
5. Yang, J.-N., "On the Normality and Accuracy of Simulated Random Processes," J. Sound and Vib., **26** (3), 417-428 (1973).
6. Box, G.E.P. and Jenkins, G.M., Time Series Analysis: Forecasting and Control, Holden-Day, San Francisco (1976).
7. Clang, M.K., Kwiatkowski, J.W. and Nau, R.F., "ARMA Models for Earthquake Ground Motions," Earthquake Eng. and Struct. Dynamics, **10**, 651-662 (1982).
8. Krenk, S. and Clausen, J., "On the Calibration of ARMA Processes for Simulation," Proc. IFIP WG 7.5, Springer Verlag, 243-257 (1987).
9. Franklin, J.N., "Numerical Simulation of Stationary and Non-stationary Gaussian Random Processes, SIAM Rev., **7** (1), 68-80 (1965).
10. Franklin, J.N., "The Covariance Matrix of a Continuous Auto-regressive Vector Time-Series," Ann. Math. Stat., **34**, 1259-1264 (1963).
11. Hammersley, J.M. and Handscomb, D.C., Monte Carlo Methods, Methuen, London (1964).
12. Schittkowski, K., NLPQL : A FORTRAN Subroutine Solving Constrained Non-Linear Programming Problems, Annals of Operations Research (1986).
13. Madsen, H.O., Krenk, S. and Lind, N.C., Methods of Structural Safety, Prentice-Hall (1986).
14. Sigurdsson, G., "Development of Applicable Methods for Evaluating the Safety of Off-shore Structures, Part 4," Structural Reliability Theory (24), The Univ. of Aalborg, Denmark (1987).

APPENDIX

Calculation of $f_{P,V}(a_1,a_2,\tau)$

The joint density function in eq (17) can be written

$$f_{P,V}(a_1,a_2,\tau) = \frac{\int_{-\infty}^{0}\int_{0}^{\infty} -\ddot{x}_1\ddot{x}_2\varphi_6(a_1,a_2,0,0,\ddot{x}_1,\ddot{x}_2;\ \bar{\bar{\varrho}}_1)d\ddot{x}_1d\ddot{x}_2}{\int_{-\infty}^{0}\int_{0}^{\infty} -\ddot{x}_1\ddot{x}_2\varphi_4(0,0,\ddot{x}_1,\ddot{x}_2;\ \bar{\bar{\varrho}}_2)d\ddot{x}_1d\ddot{x}_2} = \frac{A}{B} \tag{A1}$$

where $\varphi_n(\cdot\,,\ \bar{\bar{\varrho}})$ is the n-dimensional normalized normal density function of n variables having the correlation coefficient matrix $\bar{\bar{\varrho}}$. $\bar{\bar{\varrho}}_1$ is written

$$\bar{\bar{\varrho}}_1 = \left(\begin{array}{cccc|cc} 1 & \varrho(\tau) & 0 & \varrho^1(\tau) & \varrho^2(0) & \varrho^2(\tau) \\ \varrho(\tau) & 1 & -\varrho^1(\tau) & 0 & \varrho^2(\tau) & \varrho^2(0) \\ 0 & -\varrho^1(\tau) & -\varrho^2(0) & -\varrho^2(\tau) & 0 & -\varrho^3(\tau) \\ \varrho^1(\tau) & 0 & -\varrho^2(\tau) & -\varrho^2(0) & \varrho^3(\tau) & 0 \\ \hline \varrho^2(0) & \varrho^2(\tau) & 0 & \varrho^3(\tau) & \varrho^4(0) & \varrho^4(\tau) \\ \varrho^2(\tau) & \varrho^2(0) & -\varrho^3(\tau) & 0 & \varrho^4(\tau) & \varrho^4(0) \end{array}\right) = \left(\begin{array}{cc} \bar{\bar{\varrho}}_{11} & \bar{\bar{\varrho}}_{12} \\ \bar{\bar{\varrho}}_{12}^{\,T} & \bar{\bar{\varrho}}_{22} \end{array}\right) \tag{A2}$$

A can be written

$$A = -\varphi_4(a_1,a_2,0,0;\ \bar{\bar{\varrho}}_{11})\int_{-\infty}^{0}\int_{0}^{\infty}\ddot{x}_1\ddot{x}_2\varphi_2(\ddot{x}_1-\mu_1,\ \ddot{x}_2-\mu_2;\ \bar{\bar{R}})d\ddot{x}_1d\ddot{x}_2 =$$

$$-\varphi_4(a_1,a_2,0,0;\ \bar{\bar{\varrho}}_{11})\lambda_1\lambda_2\left[-\Psi_2\left(-\frac{\mu_1}{\lambda_1}\right)\Psi_1\left(-\frac{\mu_2}{\lambda_2}\right)\right.$$

$$\left.-\varkappa\Phi\left(-\frac{\mu_1}{\lambda_1}\right)\Phi\left(\frac{\mu_2}{\lambda_2}\right)+\lambda_1\lambda_2\int_0^{\varkappa}(\varkappa-k)\varphi_2(0,0;\ \bar{\bar{R}}(k))dk\right] \tag{A3}$$

where

$$\bar{\mu} = \left(\begin{array}{c}\mu_1\\ \mu_2\end{array}\right) = \bar{\bar{\varrho}}_{12}^{\,T}\,\bar{\bar{\varrho}}_{11}^{-1}\left(\begin{array}{c}a_1\\ a_2\\ 0\\ 0\end{array}\right) \tag{A4}$$

$$\bar{\bar{R}}(\varkappa) = \bar{\bar{\varrho}}_{22} - \bar{\bar{\varrho}}_{12}^{\,T}\,\bar{\bar{\varrho}}_{11}^{-1}\,\bar{\bar{\varrho}}_{12} = \left(\begin{array}{cc}\lambda_1^2 & \varkappa\lambda_1\lambda_2\\ \varkappa\lambda_1\lambda_2 & \lambda_2^2\end{array}\right)$$

$$\Psi_1(x) = \varphi(x) - x\Phi(x) \tag{A6}$$

$$\Psi_2(x) = -\varphi(x) - x\Phi(x) \tag{A7}$$

$\Phi(\cdot)$ is the standard normal distribution function. λ_1, λ_2 and $\varkappa$ are defined by eq (A5). ϱ_2 is written

$$\bar{\bar{\varrho}}_2 = \left(\begin{array}{cc|cc} -\varrho^2(0) & -\varrho^2(\tau) & 0 & -\varrho^3(\tau) \\ -\varrho^2(\tau) & -\varrho^2(0) & \varrho^3(\tau) & 0 \\ \hline 0 & \varrho^3(\tau) & \varrho^4(0) & \varrho^4(\tau) \\ -\varrho^3(\tau) & 0 & \varrho^4(\tau) & \varrho^4(0) \end{array}\right) = \left(\begin{array}{cc} \bar{\bar{r}}_{11} & \bar{\bar{r}}_{12} \\ \bar{\bar{r}}_{12}^{\,T} & \bar{\bar{r}}_{22} \end{array}\right) \tag{A8}$$

B in eq (A1) can then be written

$$B = -\varphi_2(0,0;\ \bar{\bar{r}}_{11})\int_{-\infty}^{0}\int_{0}^{\infty}\ddot{x}_1\ddot{x}_2\varphi_2(\ddot{x}_1,\ddot{x}_2;\ \bar{\bar{r}})d\ddot{x}_1d\ddot{x}_2$$

$$= -\varphi_2(0,0;\ \bar{\bar{r}}_{11})\lambda_1\lambda_2\left[-\Psi_2(0)\Psi_1(0)\right.$$

$$\left.-\frac{\varkappa}{4}+\lambda_1\lambda_2\int_0^{\varkappa}(\varkappa-k)\varphi_2(0,0;\ \bar{\bar{r}}(k))dk\right] \tag{A9}$$

where

$$\bar{\bar{r}}(\varkappa) = \bar{\bar{r}}_{22} - \bar{\bar{r}}_{12}^{\,T}\,\bar{\bar{r}}_{11}^{-1}\,\bar{\bar{r}}_{12} = \left(\begin{array}{cc}\lambda_1^2 & \varkappa\lambda_1\lambda_2\\ \varkappa\lambda_1\lambda_2 & \lambda_2^2\end{array}\right)$$